

QED radiative correction for the single- W production using a parton shower method

Y. Kurihara¹, J. Fujimoto¹, T. Ishikawa¹, Y. Shimizu¹, K. Kato², K. Tobimatsu², T. Munehisa³

¹ High Energy Accelerator Research Organization, Tsukuba, 305-0801, Japan

² Kogakuin University, Shinjuku, Tokyo 163-8677, Japan

³ Yamanashi University, Yamanashi 400-8510, Japan

Received: 22 February 2001 /

Published online: 11 May 2001 – © Springer-Verlag / Società Italiana di Fisica 2001

Abstract. A parton shower method for the photonic radiative correction is applied to single W -boson production processes. The energy scale for the evolution of the parton shower is determined so that the correct soft-photon emission is reproduced. Photon spectra radiated from the partons are compared with those from the exact matrix elements, and show a good agreement. Possible errors due to an inappropriate energy-scale selection or due to the ambiguity of the energy-scale determination are also discussed, particularly for the measurements on triple gauge couplings.

1 Introduction

Single- W production processes present an opportunity to study the anomalous triple gauge couplings (TGC) [1] in the experiments at LEP2 and at future e^+e^- linear colliders. For their precise predictions of cross sections the inclusion of an initial state radiative correction (ISR) is inevitable in the event-generator. As a tool for the ISR the structure function (SF) [2] and the parton shower [3] methods have been widely used for e^+e^- annihilation processes. For the case of the single- W production processes, however, the main contribution comes from non-annihilation type diagrams. The universal factorization method used for the annihilation processes is obviously inappropriate. The main problem lies in choosing the energy scale of the factorization. A previous study of the two photon process [4] has shown that the SF and QED parton shower (QEDPS) methods are able to reproduce precisely the exact $O(\alpha)$ results even for non-annihilation processes, as long as the appropriate energy scale is used.

In this report, a general method to find the energy scale for SF and QEDPS is proposed. Then numerical results of testing SF and QEDPS for $e^-e^+ \rightarrow e^- \bar{\nu}_e u \bar{d}$ and $e^-e^+ \rightarrow e^- \bar{\nu}_e \mu^+ \nu_\mu$ are presented. Systematic errors are also discussed.

2 Calculation method

2.1 Energy scale determination

The factorization theorem for QED radiative corrections in the leading-logarithmic approximation is valid independent of the structure of the matrix element of the kernel

process. Hence SF and QEDPS must be applicable to *any* e^+e^- scattering processes. However, the choice of the energy scale in SF and QEDPS is not a trivial matter [11]. For the simple processes considered so far, like e^+e^- annihilation and the two-photon process with only multi-peripheral diagrams, the evolution energy scale could be found by exact perturbative calculations. However, this is not always the case when more complicated processes are concerned. Hence a way to find a suitable energy scale without knowing exact loop calculations should be established somehow.

First, let us look at the general consequences of the soft photon approximation. The cross section with radiations in the soft-photon limit is given by the Born cross section multiplied by the following factor up to the double-log term [6]:

$$\frac{d\sigma_{\text{soft}}(s)}{d\Omega} = \frac{d\sigma_0(s)}{d\Omega} \quad (1)$$

$$\times \left| \exp \left[-\frac{\alpha}{\pi} \ln \left(\frac{E}{k_c} \right) \sum_{i,j} \frac{e_i e_j \eta_i \eta_j}{\beta_{ij}} \ln \left(\frac{1 + \beta_{ij}}{1 - \beta_{ij}} \right) \right] \right|^2,$$

$$\beta_{ij} = \left(1 - \frac{m_i^2 m_j^2}{(p_i \cdot p_j)^2} \right)^{1/2}, \quad (2)$$

where m_j (p_j) are the mass (momentum) of the j th charged particle, k_c is the maximum energy of the soft photon (the value to separate soft and hard photons), E the beam energy and e_j the electric charge in units of the e^+ charge. The factor η_j is -1 for the initial particles and $+1$ for the final particles. The indices (i, j) run over all the charged particles in the initial and final states.

For the two-photon process, $e^-(p_-)e^+(p_+) \rightarrow e^-(q_-)e^+(q_+)\mu^-(k_-)\mu^+(k_+)$, it is shown in [4] that the soft-photon factor in (1) with a $(p_- \cdot q_-)$ -term reproduces the $O(\alpha)$ corrections [7] up to the double-log term in the soft-photon limit. This implies that one is able to read off the possible evolution energy scale in SF from (1) without doing explicit loop calculations¹. The point is the observation that the energy scale $s = (p_- + p_+)^2$ does not appear in the soft-photon corrections even if they are included in the general formula (1). In the case of the two-photon process we have ignored those terms in SF which come from the photon bridging between different charged lines, because the contributions from the box diagrams with photon exchange between e^+ and e^- is known to be small [9]. Fortunately, the infrared part of the loop corrections is already included in (1) and there is no need to know the full form of the loop diagram. Let us look at two terms with, for example, $(p_- \cdot p_+)$ - and $(q_- \cdot p_+)$ -terms. The momentum of e^- is almost the same before and after the scattering ($p_- \approx q_-$). Only the difference appears in $\eta_j \eta_k = +1$ for a $(p_- p_+)$ -term and $\eta_j \eta_k = -1$ for a $(q_- p_+)$ -term. Then these terms compensate each other after summing them up for the forward scattering, which is the dominant kinematical region of this process. This is the mechanism making that the energy scale $s = (p_- + p_+)^2$ does not appear in the soft-photon correction despite that it exists in (1).

When some experimental cuts are imposed, for example when the final e^- is tagged in a large angle, this cancellation is not perfect but partial, and the energy scale s must appear in the soft-photon correction. In this case, the annihilation type diagrams will also give a contribution. Then it may happen that the usual SF and QEDPS for the annihilation processes can be justified to be to be used for the ISR with the energy scale s . To find the most dominant energy scale under the given experimental cuts an easy way is to integrate numerically the soft-photon cross section given by (1) over the allowed kinematical region. Thus, in order to determine the energy scale it is sufficient to know the infrared behavior of the radiative process using the soft-photon factor.

Let us determine the energy scale of the QED radiative corrections to the single- W production process,

$$\begin{aligned} e^-(p_-) + e^+(p_+) \\ \rightarrow e^-(q_-) + \bar{\nu}_e(q_\nu) + u(k_u) + \bar{d}(k_d). \end{aligned} \quad (3)$$

The soft-photon correction factor in (1) is numerically integrated with the Born matrix element of the process (3) only with the t -channel diagrams without any cut on the final fermions. In order to separate the contribution from each term, we take terms up to $O(\alpha)$ in the Taylor expansion of the exponential function in (1). Parameters used in the calculation will be explained in Sect. 4. The results are shown in Table 1. One can see that the main contribution comes from an electron charged line ($p_- q_-$ -term) and a positron charged line ($p_+ k_u k_d$ -terms = $p_+ k_u$ -term + $p_+ k_d$ -term + $k_u k_d$ -term), while all other contributions

Table 1. Soft-photon correction factor from sets of charged particle combinations for the process of $e^+e^- \rightarrow e^- \bar{\nu}_e u \bar{d}$ at the CM energy of 200 GeV. The factor from all terms is normalized to unity. $k_c = 1$ GeV is used. We have $p_+ k_u k_d = p_+ k_u$ -term + $p_+ k_d$ -term + $k_u k_d$ -term

All terms	$p_- q_-$	$p_+ k_u k_d$	All other combinations
1	0.38	0.61	1.9×10^{-3}

are negligibly small. Like for the two-photon processes the energy scale s does not appear in the soft-photon correction.

The above results clearly indicate that one should apply SF or QEDPS to the electron and positron charged lines individually with the energy scale of their momentum-transfer squared.

2.2 Structure function method

The analytic solution of the DGLAP evolution function [10] in the leading-logarithmic order is known as the structure function [2]. With SF the QED corrected cross section is given by

$$\begin{aligned} \sigma_{\text{total}}(s) = \int dx_{I-} \int dx_{F-} \int dx_{I+} \int dx_u \int dx_d \\ \times D_{e^-}(x_{I-}, -t_-) D_{e^-}(x_{F-}, -t_-) D_{e^+}(x_{I+}, -t_+) \\ \times D_u(x_u, s_{ud}) D_d(x_d, s_{ud}) \sigma_0(\hat{s}), \end{aligned} \quad (4)$$

where σ_0 is the Born cross section and the D 's are the SF. The energy scales $t_- = (p_- - q_-)^2$, $t_+ = (p_+ - (k_u + k_d))^2$ and $s_{ud} = (k_u + k_d)^2$ are chosen following the result of the former section. After (before) the photon radiation the initial (final) momenta p_\pm (q_\pm) become \hat{p}_\pm (\hat{q}_\pm); we have

$$\hat{p}_- = x_{I-} p_-, \quad \hat{q}_- = \frac{1}{x_{F-}} q_-, \dots \quad (5)$$

respectively. Then the CM energy squared, s , is scaled as $\hat{s} = x_{I-} x_{I+} s$.

2.3 Parton shower method

Instead of the analytic formula of SF, a Monte Carlo method based on the parton shower algorithm in QED can be used to solve the DGLAP equation in the LL approximation. Its detailed algorithm for the QEDPS is found in [12] for e^+e^- annihilation processes, in [13] for the Bhabha process, and in [4] for the two-photon process. The same energy scale as the SF method is used in QEDPS also.

A significant difference between SF and QEDPS is that the QEDPS can treat the transverse momentum of the emitted photons correctly by imposing the exact kinematics at the $e \rightarrow e\gamma$ splitting. It does not affect the total cross sections so much when the final e^- has no cut. However, the finite recoiling of the final e^\pm can result in some effects on the tagged cross sections.

¹ A similar idea is independently proposed by Montagna et al. in [8]

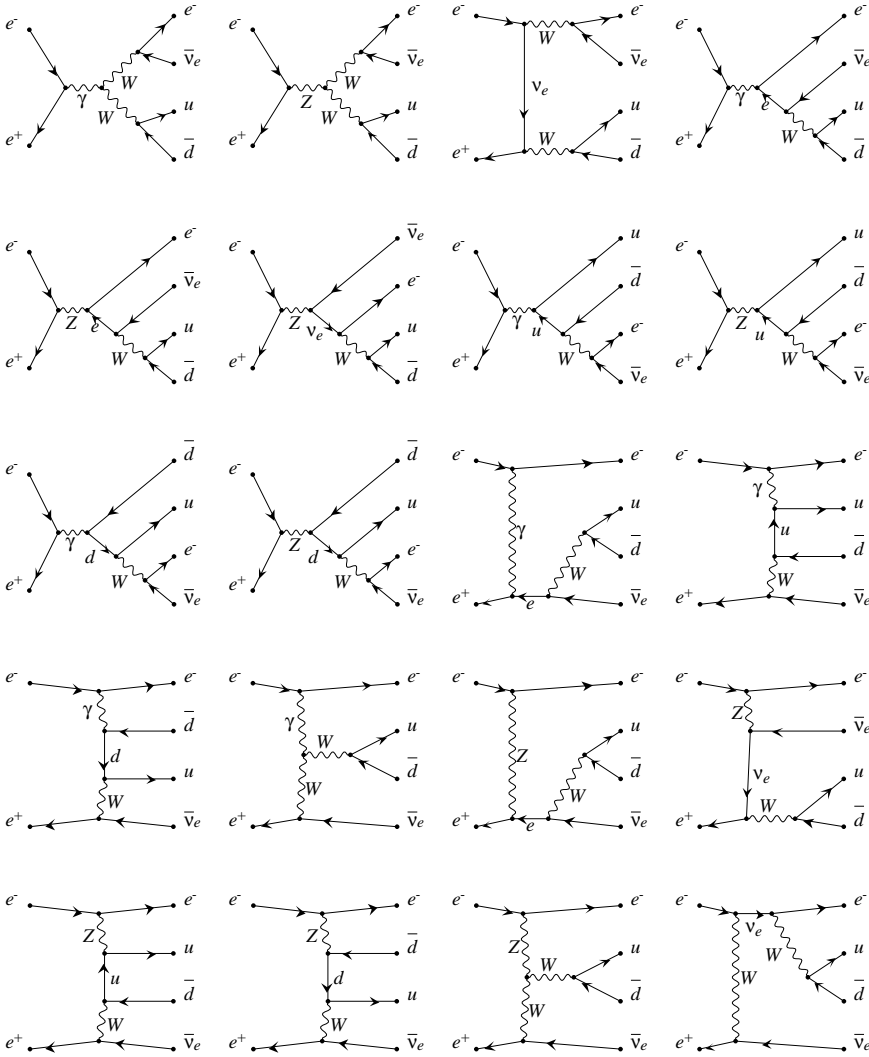


Fig. 1. Feynman diagrams of the process $e^-e^+ \rightarrow e^-\bar{\nu}_e u\bar{d}$. The first ten diagrams show the s -channel diagrams and the last ten the t -channel ones

In return for the exact kinematics at the $e \rightarrow e\gamma$ splitting, the e^\pm are no longer on shell after the emission of a photon. On the other hand, the matrix element of the hard scattering process must be calculated with on-shell external particles. A trick to map the off-shell four-momenta of the initial e^\pm to those on shell is needed. The following method is used in the calculations.

1. $\hat{s} = (\hat{p}_- + \hat{p}_+)^2$ is calculated, where \hat{p}_\pm are the four-momenta of the initial e^\pm after the photo-emission by QEDPS. \hat{s} is positive even for the off-shell e^\pm .
2. New four-momenta of the initial e^\pm in their rest-frame, \tilde{p}_\pm , are defined by $\tilde{p}_\pm^2 = m_e^2$ (on shell) and $\hat{s} = (\tilde{p}_- + \tilde{p}_+)^2$. All four-momenta of the final particles are generated in the rest-frame of $\tilde{p}_+ + \tilde{p}_-$.
3. All four-momenta are rotated and boosted to match the three-momenta of \tilde{p}_\pm with those of \hat{p}_\pm .

This method respects the direction of the final e^\pm rather than the CM energy of the collision. The total energy is not conserved in this case because of the virtuality of the initial e^\pm . The violation of the energy conservation is of the order of 10^{-6} GeV or less, and the probability of a violation of more than 1 MeV is 10^{-4} .

3 Numerical calculations

3.1 Cross sections with no cut

Total and differential cross sections of the semi-leptonic process $e^-e^+ \rightarrow e^-\bar{\nu}_e u\bar{d}$ and the leptonic process $e^-e^+ \rightarrow e^-\bar{\nu}_e \mu^+ \nu_\mu$ are calculated with the radiative correction by SF or QEDPS. Feynman diagrams of the semi-leptonic process are shown in Fig. 1. Fortran codes to calculate the amplitudes are automatically produced by the GRACE system [14]. All fermion masses are kept finite in the calculations. Numerical integrations of the matrix element squared in the four-body phase space are done using BASES [15]. For a test with no experimental cuts, only the t -channel diagrams (non-annihilation diagrams) are taken into account. Standard model parameters used in the calculations are summarized in Table 2. The on-shell relation that strictly holds at tree level is employed to determine the weak couplings. Some of the electroweak corrections could be taken into account through the G_μ -scheme and the running coupling constant. In this report, however, we do not include those effects, because here we are interested

Table 2. Standard model parameters

M_W	80.35 GeV	Γ_W	1.96708 GeV
M_Z	91.1867 GeV	Γ_Z	2.49471 GeV
α	1/137.0359895	$\sin^2 \theta_w$	$1 - \frac{M_W^2}{M_Z^2}$
m_e	0.511×10^{-3} GeV	m_μ	$105.658389 \times 10^{-3}$ GeV
m_u	5.0×10^{-3} GeV	m_d	10.0×10^{-3} GeV

in looking at the pure QED radiative corrections to the Born cross section.

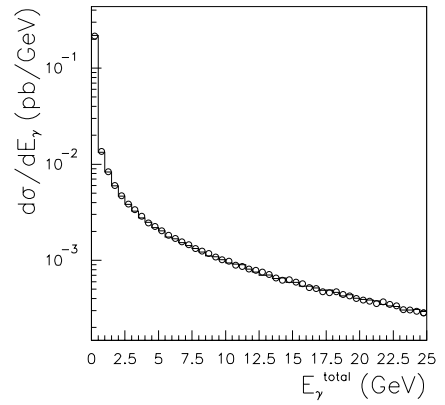
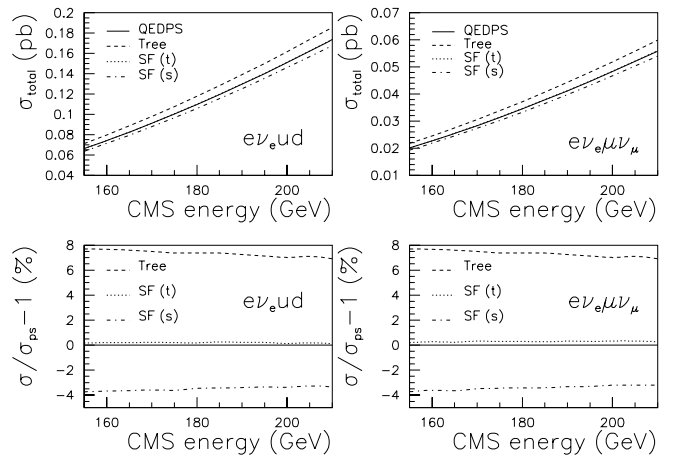
It has been pointed out that a tiny violation of the gauge invariance caused by the inclusion of a finite W -boson width results in a wrong cross section for single- W production [16,17]. To cure this problem the fermion-loop scheme [17–19] has been proposed. It is reported in [18], however, that no significant difference is seen between the fermion-loop scheme and the fixed width scheme. Thus, in this report the fixed width scheme, together with an appropriately modified current described in [16] is employed.

For the total energy of the emitted photons, both methods, SF and QEDPS, must give the same spectrum once the same energy scale is used. This is confirmed for the semi-leptonic process as shown in Fig. 2 at the CM energy of 200 GeV. We choose the same energy-evolution scale as SF described by (4). Total cross sections as a function of the CM energies at LEP2 with no cuts are shown in Fig. 3. The effects of the QED radiative corrections on the total cross sections are found to be 7 to 8% in the LEP2 energy region. If one used an inappropriate energy scale, say s , in SF, the ISR effect is overestimated by about 4% as seen in Fig. 3. The result of SF is consistent with the QEDPS to around 0.2% if the proper energy scale is employed.

There is some ambiguity in the choice of the energy-evolution scale in the leading-log order. For example, the transverse-momentum squared or the invariant-mass squared of $u\bar{d}$ (or the $\mu\bar{\nu}_\mu$) systems could be a candidate for the energy scale. It is found that even if these energy scales are chosen in QEDPS instead of $(p_+ - (k_u + k_d))^2$, the total cross sections change by only 0.6%, which must be allocated in the theoretical uncertainty.

The energy and angular distributions of the hard photon from QEDPS are compared with those obtained from the exact matrix elements. The cross sections of the radiative process $e^-e^+ \rightarrow e^-\bar{\nu}_e u\bar{d}\gamma$ are calculated based on the exact amplitudes generated by GRACE and integrated numerically in five-body phase space using BASES. Again only the t -channel diagrams (non-annihilation diagrams) are taken into account. To compare the distributions the soft-photon corrections for the radiative process must be included. For this purpose QEDPS is implemented into the $e^-\bar{\nu}_e u\bar{d}\gamma$ calculations carefully avoiding a double-counting of the radiation effect. The definition of the hard photon is

1. $E_\gamma > 1$ GeV;
2. the opening angle between the photon and the nearest final-state charged particles is greater than 5° . The dis-

**Fig. 2.** Differential cross section and the total energy of emitted photon(s) obtained from the QEDPS (histogram) and from the SF (circle)**Fig. 3.** Total cross sections and those normalized by the QEDPS results for $e\nu_e\bar{u}d$ and $e\nu_e\mu\nu_\mu$ processes without experimental cuts. The SF(t) denotes the SF with proper energy scale and the SF(s) with the inappropriate energy scale (s). Only t -channel diagrams (non-annihilation diagrams) are taken into account

tributions of the hard photons are in good agreement, as seen in Fig. 4. The total cross section of the hard-photon emission agrees at the 2% level. We also calculated the radiative cross section without soft-photon correction. If the soft-photon correction is not included in the radiative process, we find a 30% overestimation of the radiative cross section with the above experimental cuts.

3.2 Cross sections with experimental cut

It is also investigated how large the effects of the QED radiative corrections are for the single- W production when realistic experimental conditions are imposed. The experimental cuts applied here are $\theta_{e^-} < 5^\circ$, $M_{q\bar{q}} > 45$ GeV, $E_\mu > 20$ GeV. For this study all the diagrams, not only the t -channel diagrams, but also the s -channel, are taken into account in the calculations. The dominance of the signal

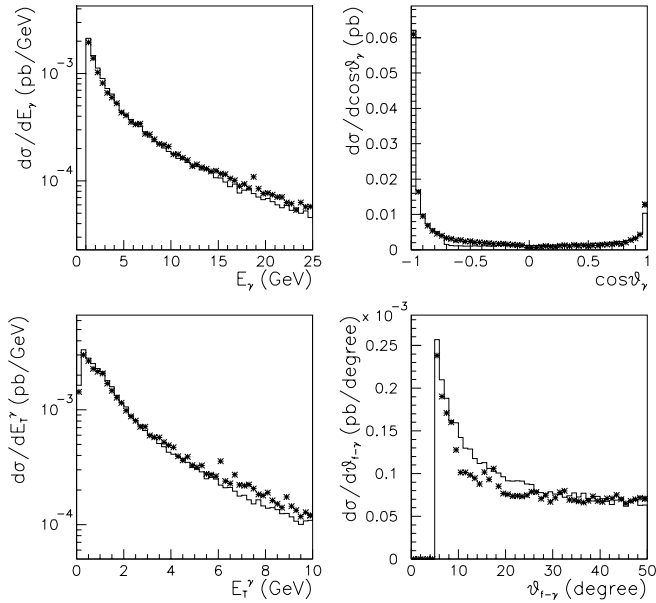


Fig. 4. Differential cross sections of the hard photon; energy, transverse energy with respect to the beam axis, cosine of the polar angle, and opening angle between photon and nearest charged fermion. A histogram shows the QEDPS result and stars results from the matrix element with soft-photon correction. Only t -channel diagrams (non-annihilation diagrams) are taken into account

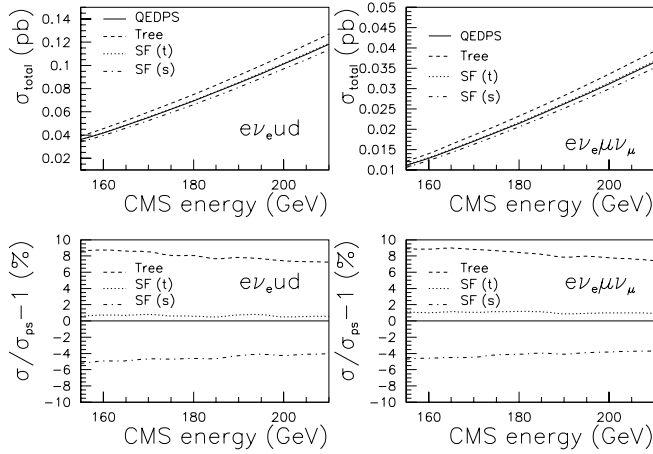


Fig. 5. Total cross sections and those normalized by the QEDPS results for $e\nu_e\bar{u}$ and $e\nu_e\mu\nu$ processes with experimental cuts. The SF(t) denotes the SF with proper energy scale and the SF(s) with the inappropriate energy scale (s). All diagrams are taken into account

from t -channel diagrams is 97% (90%) for the hadronic (leptonic) decay of the W -boson, respectively. Total cross sections as a function of the CM energies at LEP2 with these cuts are shown in Fig. 5. The QED radiative corrections on the total cross sections are found to be 7 to 8% in this LEP2 energy range. If one uses the inappropriate energy scale s in SF, the ISR effect is overestimated by around 5%, which is larger than those of the no-cut case. SF with the proper energy scale shows a deviation from

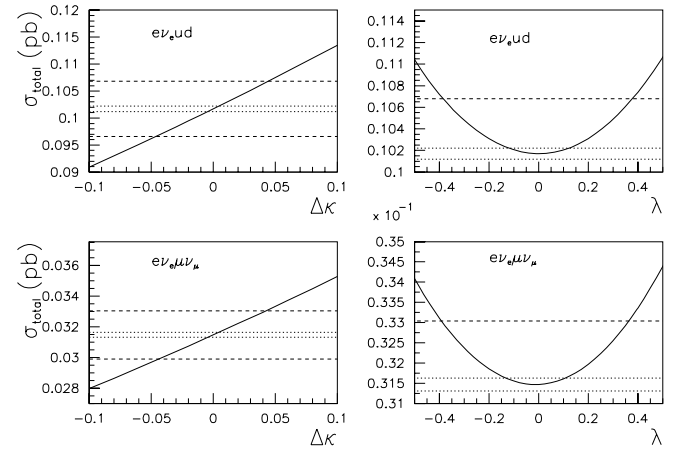


Fig. 6. Total cross sections of $e\nu_e\bar{u}$ and $e\nu_e\mu\nu$ processes with experimental cuts as a function of the anomalous TGC. Dashed (dotted) lines show $\pm 5\%$ ($\pm 0.6\%$) cross section variation from its standard model value. The cross sections are obtained at the CM energy of 200 GeV with all diagrams

QEDPS around 0.5% for the $e^-\bar{\nu}_e\bar{u}$ process and 1.0% for $e^-\bar{\nu}_e\mu^+\nu_\mu$. The agreement between QEDPS and SF becomes worse than the no-cut case, because the finite transverse momentum of the emitted photons by QEDPS changes the acceptance of the above electron-veto requirement. Hence for realistic experimental conditions the finite transverse momentum of the emitted photons should not be ignored.

Finally, a possible effect of the systematic error of the ISR effect on the anomalous TGC measurements is investigated. If the inappropriate energy scale is used in the ISR tools such as the CM energy squared, the total cross sections with the experimental cuts includes a systematic error of 5%. Even if one used one of the proper energy scales, there is 0.6% uncertainty on the cross sections due to the ambiguity of the energy scale selection. This uncertainty of the total cross sections limits the experimental sensitivity of the anomalous TGC measurements. The total cross sections of the $e\nu_e\bar{u}$ and $e\nu_e\mu\nu$ processes with experimental cuts as a function of the anomalous TGC are summarized in Fig. 6. The cross sections are obtained at the CM energy of 200 GeV in all diagrams. A bound shown in dashed lines shows a $\pm 5\%$ cross section variation from its standard model value. If one used the inappropriate energy scale, it affects ± 0.05 of the $\Delta\kappa$ measurement and ± 0.4 of the λ measurement. The ambiguity of the energy-scale selection gives a systematic error of less than 0.01 on $\Delta\kappa$ and 0.1 on λ .

4 Conclusions

The method to apply the QED radiative correction to the non-annihilation process was established. The conventional method, SF with the energy scale s , gave about 4% overestimation in the LEP2 energies. The uncertainty due to the energy-scale determination was estimated to be about 0.6%. This uncertainty may affect the anoma-

lous TGC measurements by less than 0.01 on $\Delta\kappa$ and 0.1 on λ . If one wants to look at the hard-photon spectrum, the soft-photon corrections to these radiative processes are needed.

In this report we have treated the two processes $e^-e^+ \rightarrow e^-\bar{\nu}_e u \bar{d}$ and $e^-e^+ \rightarrow e^-\bar{\nu}_e \mu^+ \nu_\mu$. The CP -conjugate processes $e^-e^+ \rightarrow e^+\nu_e \bar{u} d$ and $e^-e^+ \rightarrow e^+\nu_e \mu^- \bar{\nu}_\mu$ give the same results, and the other channels, $e^-e^+ \rightarrow e\nu_e c s$ and $e^-e^+ \rightarrow e\nu_e \tau \nu_\tau$, will show slightly different results due to their masses. On the other hand the self- CP -conjugate process $e^-e^+ \rightarrow e^-\bar{\nu}_e e^+ \nu_e$ has an additional complexity, because the two energy scales $t_- = (p_{e^-} - q_{e^-})^2$ and $\tilde{t}_- = (p_{e^-} - q_{e^-} - q_{\bar{\nu}_e})^2$ can occur simultaneously.

Acknowledgements. The authors would like to thank the members of the four-fermion working group of the LEP2 Monte Carlo Workshop at CERN, in particular A. Ballesterero, G. Montagna, F. Piccinini and G. Passarino, for useful discussions. This work was supported in part by the Ministry of Education, Science and Culture under the Grant-in-Aid No. 11206203 and 11440083.

References

1. T. Tsukamoto, Y. Kurihara, Phys. Lett. B **389**, 162 (1996)
2. E.A. Kuraev, V.S. Fadin, Sov. J. Nucl. Phys. **41**, 466 (1985); G. Altarelli, G. Martinelli, in Physics at LEP, edited by J. Ellis, R. Peccei, CERN 86-02 (CERN, Geneva 1986); O. Nicrosini, L. Trentadue, Phys. Lett. B **196**, 551 (1987); Z. Phys. C **39**, 479 (1988); F.A. Berends, G. Burgers, W.L. van Neerven, Nucl. Phys. B **297**, 429 (1988)
3. G. Marchesini, B.R. Webber, Nucl. Phys. B **238**, 1 (1984); R. Odorico, Nucl. Phys. B **172**, 157 (1980); T. Sjöstrand, Comput. Phys. Commun. **79**, 503 (1994)
4. Y. Kurihara, J. Fujimoto, Y. Shimizu, K. Kato, K. Tobimatsu, T. Munehisa, Prog. Theor. Phys. **103**, 1199 (2000)
5. W. Beenakker, F.A. Berends, W.L. van Neerven, Proceedings of Radiative Correction for e^+e^- Collisions, edited by J.H. Kühn (Springer-Verlag, Heidelberg 1989), p. 3
6. F. Bloch, A. Nordsieck, Phys. Rev. **37**, 54 (1937); D.R. Yennie, S.C. Frautschi, H. Suura, Ann. Phys. **13**, 379 (1961); see also S. Weinberg, The quantum theory of fields (Cambridge University Press, New York 1995), Sect. 13
7. F.A. Berends, P.H. Daverveldt, R. Kleiss, Nucl. Phys. B **253**, 412 (1985)
8. G. Montagna, M. Moretti, O. Nicrosini, A. Pallavicini, F. Piccinini, hep-ph/0005121
9. W.L. van Neerven, J.A.M. Vermaseren, Nucl. Phys. B **238**, 73 (1984); W.L. van Neerven, J.A.M. Vermaseren, Phys. Lett. B **137**, 241 (1984); W.L. van Neerven, J.A.M. Vermaseren, NIKHEF Amsterdam preprint 84-2 (1984)
10. V.N. Gribov, L.N. Lipatov, Sov. J. Nucl. Phys. **15**, 298 (1972); G. Altarelli, G. Parisi, Nucl. Phys. B **126**, 298 (1977); Y.L. Dokshitzer, Sov. Phys. JETP **46**, 641 (1977)
11. W. Beenakker, F.A. Berends, W.L. van Neerven, Proceedings of Radiative Correction for e^+e^- Collisions, edited by J.H. Kühn (Springer-Verlag, Heidelberg 1989), p. 3
12. T. Munehisa, J. Fujimoto, Y. Kurihara, Y. Shimizu, Prog. Theor. Phys. **95**, 375 (1996)
13. J. Fujimoto, Y. Shimizu, T. Munehisa, Prog. Theor. Phys. **91**, 333 (1994); K. Tobimatsu, in preparation
14. T. Ishikawa, T. Kaneko, K. Kato, S. Kawabata, Y. Shimizu, H. Tanaka, KEK Report 92-19, 1993, The GRACE manual Ver. 1.0; see also H. Tanaka, Comput. Phys. Commun. **58**, 153 (1990); H. Tanaka, T. Kaneko, Y. Shimizu, Comput. Phys. Commun. **64**, 149 (1991)
15. S. Kawabata, Comp. Phys. Commun. **41**, 127 (1986); *ibid.*, **88**, 309 (1995)
16. Y. Kurihara, D. Perret-Gallix, Y. Shimizu, Phys. Lett. B **349**, 367 (1995)
17. E.N. Argyres et al., Phys. Lett. B **358**, 339 (1995); W. Beenakker et al., Nucl. Phys. B **500**, 255 (1997)
18. E. Accomando, A. Ballesterero, E. Maina, Phys. Lett. **479**, 162 (2000)
19. G. Passarino, hep-ph/9911482 and hep-ph/0001212